

# Coexistence of normal, super-, and hyper-deformation in nuclei: A study with angular momentum projection

Yang Sun <sup>a,b</sup>, Jing-ye Zhang <sup>c</sup>, Gui-Lu Long <sup>d,e</sup>, Cheng-Li Wu <sup>f</sup>

<sup>a</sup>*Department of Physics, Shanghai Jiao Tong University, Shanghai 200240, P. R. China*

<sup>b</sup>*Joint Institute for Nuclear Astrophysics, University of Notre Dame, Notre Dame, Indiana 46556, USA*

<sup>c</sup>*Department of Physics and Astronomy, University of Tennessee, Knoxville, Tennessee 37996, USA*

<sup>d</sup>*Department of Physics, Tsinghua University, Beijing 100084, P.R. China*

<sup>e</sup>*Center of Nuclear Theory, Lanzhou National Laboratory of Heavy Ion Accelerator, Lanzhou 730000, P. R. China*

<sup>f</sup>*Department of Physics, Chung Yuan Christian University, Chung-Li, Taiwan 32023, ROC*

---

## Abstract

Angular-momentum-projected energy surface calculations for  $A \approx 110$  nuclei indicate three distinct energy minima occurring at different angular-momenta. These correspond to normal, super-, and hyper-deformed shapes coexisting in one nucleus.  $^{110}\text{Pd}$  is studied in detail, with a quantitative prediction on super- and hyper-deformed spectra by the Projected Shell Model calculation. It is suggested that several other neighboring nuclei in the  $A$ -110 mass region, with the neutron number around 64, also exhibit clear super- and hyper-deformation minima.

*Key words:* nuclear shapes, hyper-deformation, angular momentum projection

*PACS:* 21.10.Re, 21.60.-n, 27.60.+j

---

## 1 Introduction

The usual assumption of nuclear structure models is that a nucleus can be described as a set of interacting particles moving in an average potential. The nucleonic motion in a potential well often occurs in a highly coherent way, giving

rise to collective phenomena such as rotational spectra and large quadrupole moments. These led to the idea of introduction of the concept of nuclear deformation [1]. Since then, the search for exotic nuclear shapes has continuously been one of the research frontiers in nuclear structure physics. One remarkable example is the discovery of super-deformed (SD) rotational bands [2]. Moreover, microscopic calculations [3,4,5,6] have predicted that some nuclei may attain even greater quadrupole deformations corresponding to a hyper-deformed (HD) shape, and that the nuclei with these deformations are possibly stable against nuclear fission. Experimentally, the search for HD states has been continued for years (see, for example, Ref. [7] and conference proceedings of the 2004 Zakopane School [8]).

The observation of rotational bands in  $^{108}\text{Cd}$  has stimulated a new wave of study along this line. In Ref. [9], Clark *et al.* reported a rotational band with the data indicating that this nucleus has the most deformed shape identified to date. Using the Projected Shell Model (PSM) [10], some of us analyzed the structure of the band. It was found [11] that the wavefunctions of the observed states notably contain a component of the proton  $i_{13/2}$  orbital from the  $N = 6$  harmonic oscillator shell. It is well-known that the  $\pi i_{13/2}$  orbitals usually appear near the proton Fermi level in normal-deformed (ND) nuclei of the actinide region, and near those in SD nuclei of the rare-earth region. In a  $Z = 48$  nucleus of the  $A=110$  mass region, occupation of the  $\pi i_{13/2}$  orbitals is possible only if the nucleus has a greater deformation.

Inspired by these advances, we have employed the PSM to carry out a systematic study on the neighboring nuclei of  $^{108}\text{Cd}$ . Angular-momentum-projected energy surface calculations have explored distinct minima in some of these nuclei, separately lying at different deformations and angular momenta. Based on the content of the wavefunctions, in which nucleons from several major shells contribute to the collectivity near the Fermi surface, we can understand the occurrence of the minima as a correlation effect involving multiple major shells. According to our analysis,  $^{108}\text{Cd}$  has two energy minima. The observed band in  $^{108}\text{Cd}$  [9] (with neutron number 60) belongs to the second minimum. As we shall show in the present paper, three energy minima, which correspond to ND, SD, and HD shapes coexisting in one nucleus, can be formed in nuclei with neutron number around 64.

The paper is organized as follows. In Section 2, we outline the theory and give the calculation conditions. In Section 3, we take  $^{110}\text{Pd}$  as an example to present the main results of the present study. Further quantitative predictions are given in Section 4. Finally, the paper is summarized in Section 5.

## 2 Theory of angular momentum projection

Using a conventional shell model to study deformed, heavy nuclei is desirable. However, it is unfeasible in practice because of the unavoidable problem related to huge basis dimensions. Therefore, the study of deformed, heavy nuclei has relied mainly on the mean field approximation. In a mean field theory, single particle motion is treated properly which gives rise to a correct description of shell structure. However, correlations beyond the mean field level are usually neglected. If the energy gain due to the correlations would be a constant with no particle-number and angular-momentum dependence, then consideration of correlations may not be important. However, it is often not the case in reality. As we shall see in the  $^{110}\text{Pd}$  example, when the correlation effect is added to that of shell structure, several energy minima clearly occur in the projected energy curves.

The Projected Shell Model [10] is a shell model built from a deformed basis. To be concrete, the PSM constructs its shell-model space by using the deformed Nilsson single-particle states with a deformation  $\varepsilon_2$ . Pairing correlations are incorporated into the Nilsson states by the BCS calculations. The consequence of the Nilsson-BCS calculations defines a set of quasiparticle (qp) states associated with the qp vacuum  $|\phi(\varepsilon_2)\rangle \equiv |0\rangle$  in the intrinsic frame. One then builds shell model bases by writing multi-qp states on top of  $|0\rangle$ :

$$|\Phi_\kappa\rangle = \left\{ |0\rangle, \alpha_{n_i}^\dagger \alpha_{n_j}^\dagger |0\rangle, \alpha_{p_i}^\dagger \alpha_{p_j}^\dagger |0\rangle, \alpha_{n_i}^\dagger \alpha_{n_j}^\dagger \alpha_{p_i}^\dagger \alpha_{p_j}^\dagger |0\rangle, \dots \right\}, \quad (1)$$

where  $\alpha^\dagger$  is the qp creation operator and the index  $n$  ( $p$ ) denotes neutron (proton) Nilsson quantum numbers of the orbitals. In Eq. (1), when the higher order multi-qp states denoted by “ $\dots$ ” are all included, one recovers the complete shell model configuration. In practice, these high order multi-qp states are not necessarily needed if one is interested in the near-Yrast property only. We have checked that for producing energy minima reported in the present paper, nearly the same results are obtained when the basis size in (1) is changed from a few to a few hundreds. Angular momentum projection transforms the wavefunction from the intrinsic frame to the laboratory frame. The total wavefunction is expressed as

$$|\Psi_M^I\rangle = \sum_\kappa f_\kappa^I \hat{P}_{MK\kappa}^I |\Phi_\kappa\rangle, \quad (2)$$

where  $\hat{P}^I$  is the angular-momentum-projection operator [12] and  $\kappa$  labels the basis states. Finally a two-body shell model Hamiltonian is diagonalized in the projected space, and the diagonalization determines  $f_\kappa^I$  in (2). This relatively-simple model has been extensively tested in the past decade. For the applica-

tions related to the present work, the PSM has been successful in describing the SD states in different mass regions [13,14,15,16].

In searching for energy minima, we calculate the angular-momentum-projected energy

$$E^I = \frac{\langle \Psi^I | \hat{H} | \Psi^I \rangle}{\langle \Psi^I | \Psi^I \rangle} \quad (3)$$

as a function of static quadrupole moment defined by

$$\langle Q \rangle = e_{\text{eff}} \frac{\langle \Psi^I | \hat{Q} | \Psi^I \rangle}{\langle I020 | I0 \rangle}, \quad (4)$$

where the effective charges are  $e_{\text{eff}} = 1.5e$  for protons and  $0.5e$  for neutrons. The energy  $E^I$  and the variable  $\langle Q \rangle$  are both evaluated by using the same wavefunction (2).

Equation (3) represents a study of energy minimization after angular momentum projection. In principle, the energies calculated with  $|\Psi^I\rangle$  can have advantages over those with unprojected state  $|0\rangle$  in that the projection treats the states fully quantum-mechanically by collecting all the energy-degenerate mean-field states associated with the rotational symmetry. Angular momentum projection is a superposition in the Euler space which lowers the total energy of the system. The energy gain is due to the correlations, which is particularly important in the present content for the formation of local deformation minima. Although in some cases, especially when the minima are deep and stable, the results between projected and unprojected calculations are qualitatively similar, there have been many examples with qualitatively different conclusions (as for instance, the one shown in the seminal work of Hayashi, Hara, and Ring [17]). In recent years, there have been attempts to incorporate angular-momentum-projection in the theories with effective interactions [18,19,20,21,22], and notable effects due to projection have been found.

The Hamiltonian appearing in (3) is of the quadrupole plus pairing type, with the inclusion of the quadrupole-pairing term [10]

$$\hat{H} = \hat{H}_0 - \frac{1}{2}\chi \sum_{\mu} \hat{Q}_{\mu}^{\dagger} \hat{Q}_{\mu} - G_M \hat{P}^{\dagger} \hat{P} - G_Q \sum_{\mu} \hat{P}_{\mu}^{\dagger} \hat{P}_{\mu}. \quad (5)$$

This is a rotation-invariant Hamiltonian with each term in it is a scalar. In Eq. (5),  $\hat{H}_0$  is the spherical single-particle Hamiltonian which contains a proper

Table 1  
 Quadrupole-quadrupole interaction strengths (in MeV).

	$\chi_{nn}$	$\chi_{pp}$	$\chi_{np} = \chi_{pn}$
Region I	0.0377	0.0302	0.0337
Region II	0.0355	0.0284	0.0318

spin-orbit force [23]. The monopole pairing strengths  $G_M$  are taken to be  $17.5/A$  for neutrons and  $19.5/A$  for protons, where  $A$  is the total particle number. The quadrupole pairing strength  $G_Q = 0.16G_M$ , which is the value usually taken in the PSM calculation. These parameters are found to be appropriate for a correct description of the known data. To incorporate the shell effect across a large single-particle space, nucleons in three major shells ( $N = 3, 4, 5$  for both neutrons and protons) and in four major shells ( $N = 4, 5, 6, 7$  for neutrons and  $N = 3, 4, 5, 6$  for protons) are activated, respectively, for the smaller deformation region (denoted as Region I) and for the larger deformation region (denoted as Region II). The quadrupole-quadrupole interaction strengths  $\chi$  are listed in Table I for the regions I and II, and these values are determined in a similar way as in Ref. [21].

### 3 Detailed analysis of $^{110}\text{Pd}$

In Fig. 1, we show the calculated energy surfaces for  $^{110}\text{Pd}$  with different angular momenta. The results clearly indicate three local minima appearing at distinct deformations (marked by red dots). The first minimum starts from  $\langle Q \rangle = 0.7$  eb at spin  $I = 0$ , and as spin increases, gradually moves to a higher  $\langle Q \rangle$  value of 1.0 (corresponding to a deformation of  $\varepsilon_2 \approx 0.25$ ). The change of deformation with spin indicates a softness of the system at the low angular-momentum region. At about  $I = 8$ , the shape is stabilized and the system begins to show a rotor character. We note that Regan *et al.* [24] discussed, with a collection of many experimental data in this mass region, the evolution of the rotational behavior in terms of transition from vibrational to rotational motion. Our present calculation may provide a microscopic insight to the observation, which suggests that this rotational behavior can be understood as a gradual increase in deformation with increasing spin in the first energy minimum [25].

The second minimum is located at about  $\langle Q \rangle = 2.8$  eb, corresponding to  $\varepsilon_2 \approx 0.57$ . The minimum is fully developed only at spin  $I = 24$  and above. The third one starts showing up at a rather high spin  $I \sim 44$  at about  $\langle Q \rangle = 3.9$  eb, corresponding to  $\varepsilon_2 \approx 0.79$ . Unlike the first one, the second and the third minimum are stable (*i.e.* the deformation minimum does not change with spin), reflecting a rigid-rotor character. It is worthwhile mentioning that

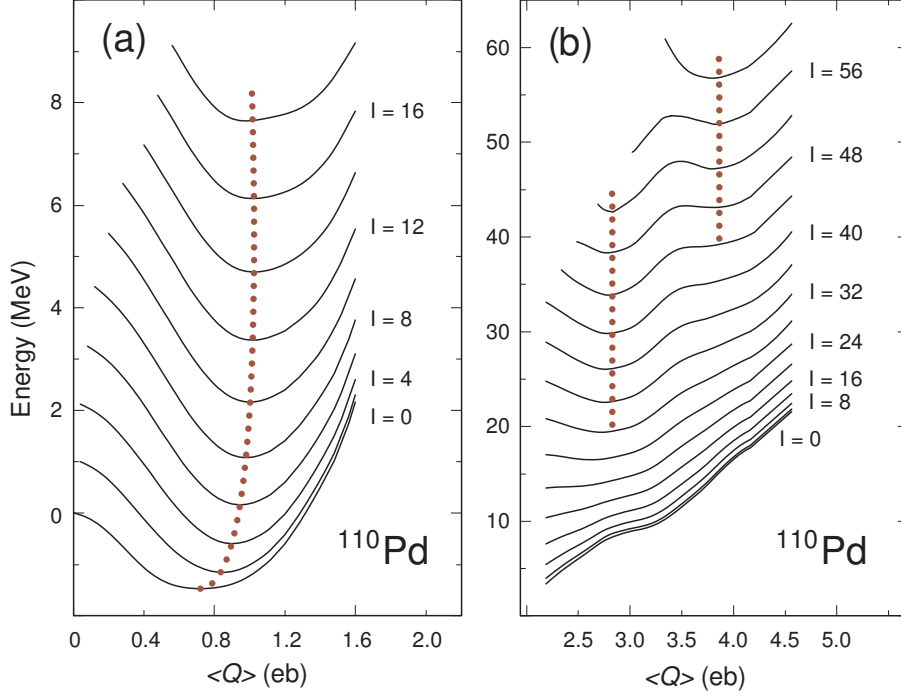


Fig. 1. Calculated energy surfaces in  $^{110}\text{Pd}$  for different angular momenta as a function of static quadrupole moment  $\langle Q \rangle$ . (a) Region I. The energy zero is set to be the total energy at  $\langle Q \rangle = \varepsilon_2 = 0$  and  $I = 0$ . (b) Region II. The absolute energy is arbitrarily chosen. Note that the plots do not give the relative energy between the two regions.

in a sharp contrast, unprojected energies (not shown in the figure) suggest a qualitatively different picture: a flat bottom centering at  $\varepsilon_2 = 0$  and only one rather shallow minimum at  $\varepsilon_2 \approx 0.67$ . We believe that this difference comes from the treatment with projection, which incorporates the many-body correlations missed in the mean-field states.

A complete description (including particle-alignment and back-bending in moment of inertia) of the ND states usually requires a mixing of the shell with the next  $N$ -shell (with the high- $j$  intruder orbitals included). Now our calculation indicates clearly that the SD and HD minima are a consequence of a shell-mixing with the next two and next three  $N$ -shells, respectively. This picture is consistent with the main conclusions of Dudek *et al.* [26,27,28]. As schematically shown in Fig. 2, the diagram exhibits a correspondence between formation of a deformed shape and an actual participation of nuclear shells in the collective motion. It is clear that formation of each higher level of deformation is associated with particles from an additional major shell in the shell mixing near the Fermi level. In our example here, the occurrence of the HD minimum in  $^{110}\text{Pd}$  requires a collective participation of four neutron shells up to the  $N = 7$ , and four proton shells up to the  $N = 6$  shell, respectively.

For a higher  $N$ -shell, it is evident that among all the orbitals, the down-

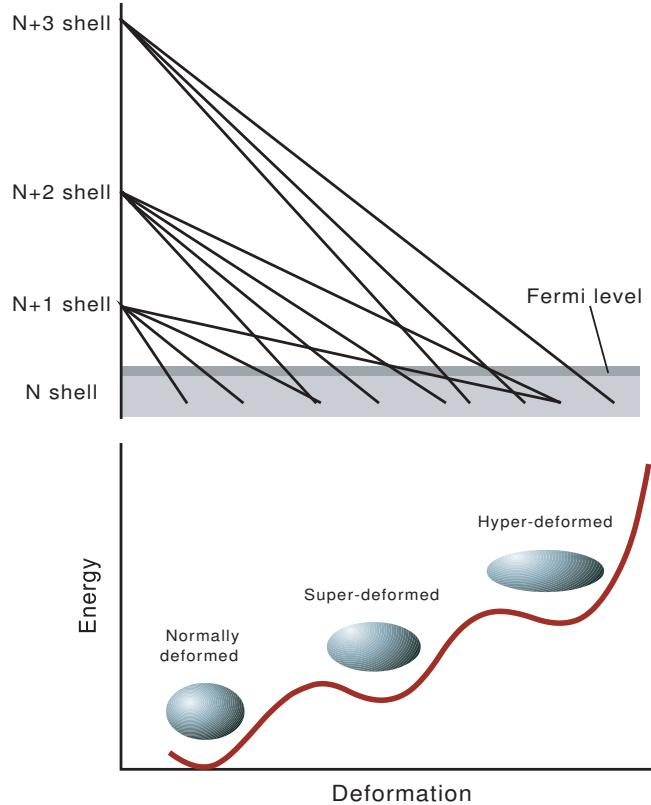


Fig. 2. Schematic diagram illustrating a correlation between a formation of deformation minima and shell mixing near the Fermi level: ND  $\leftrightarrow$  adding  $N + 1$  shell, SD  $\leftrightarrow$  adding  $N + 2$  shell, and HD  $\leftrightarrow$  adding  $N + 3$  shell.

sloping intruder orbitals with the highest  $j$  are always occupied first. It is well-known that these intruder orbitals are important in determining the nuclear high-spin behavior because of their unique properties with rotation. Thus the next question is what role these intruder orbitals play in the formation of the extreme deformation. To answer this question, we consider the expectation value of the occupation operator

$$n = \langle \Psi^I | \hat{N} = \sum_i c_i^\dagger c_i | \Psi^I \rangle. \quad (6)$$

If the summation runs only over the highest  $j$  intruder orbitals we denote it as  $n_{\text{intr}}$  (for the HD minimum,  $j_{\text{intr}}$  is  $j_{15/2}$  for neutrons and  $i_{13/2}$  for protons), otherwise as  $n_{\text{all}}$  when summing over all the orbitals of like particles. We calculate the ratio  $r = n_{\text{intr}}/n_{\text{all}}$  for each spin state by including those orbitals within  $\pm 5$  MeV around the Fermi level.

In Fig. 3, the ratio  $r$  obtained at three deformations around the HD minimum in  $^{110}\text{Pd}$  are separately shown for protons and neutrons. It can be seen that in both figures,  $r$  are rather small at  $\varepsilon_2 = 0.64$ , indicating that occupation of these intruder orbitals are not important for this deformation. However, at

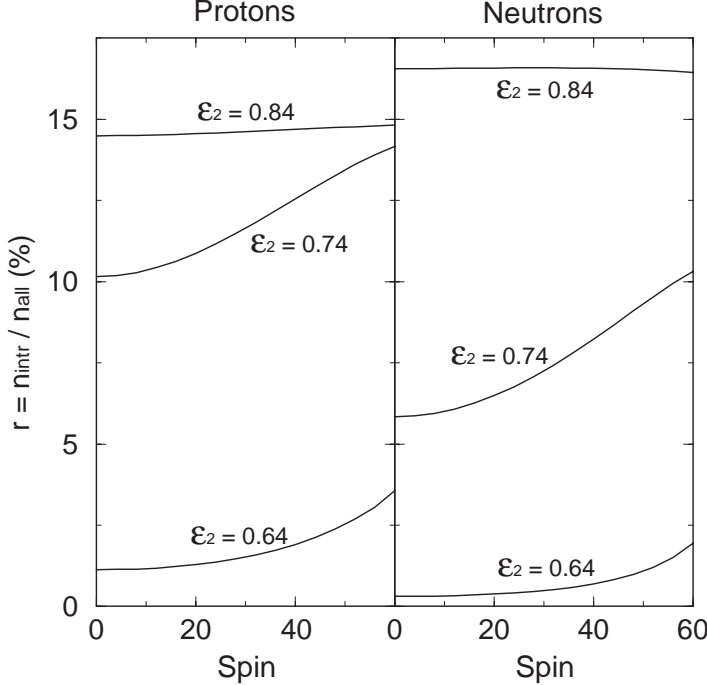


Fig. 3. Percentage of high- $j$  intruder occupation for different spin states with deformations around the HD minimum in  $^{110}\text{Pd}$ .

$\varepsilon_2 = 0.74$  where the HD minimum is about to develop, a significant increase in  $r$  is observed. In addition,  $r$  increase rapidly with spin, suggesting that the highest  $j$  intruder orbitals play a more important role in high spin states. Finally at  $\varepsilon_2 = 0.84$  beyond the HD minimum,  $r$  reaches the maxima and stay constant with spin (about 14.5% for the  $i_{13/2}$  protons, and 16.5% for the  $j_{15/2}$  neutrons). Thus roughly, the highest  $j$  intruder contributes about 1/7 to the states under discussion. This is a remarkable value, considering the fact that this amount comes from only a few intruder orbitals. On the other hand, the major part of the contribution is indeed from many particles of the rest orbits although each individual may only contribute a little.

Pairing is one of the most important correlations in nuclear states. In many high-spin calculations, however, pairing is often neglected for simplicity. By using the total wavefunction of Eq. (2), we have evaluated the pairing correlation in terms of pairing gaps

$$\Delta_\tau^I = G_M^\tau \langle \Psi^I | \hat{P}_\tau | \Psi^I \rangle. \quad (7)$$

In Eq. (7),  $\hat{P}_\tau$  is the pair operator,  $G_M^\tau$  the pairing strengths in Eq. (5), and  $\tau = \pi$  or  $\nu$ . The results for the HD states, with the corresponding wavefunctions yielding a quadrupole moment  $\langle Q \rangle = 3.9$  eb, are plotted in Fig. 4. It can be seen that the pairing gaps decrease with spin as anticipated, which has been understood as a reduction in pairing correlation due to the rotational align-

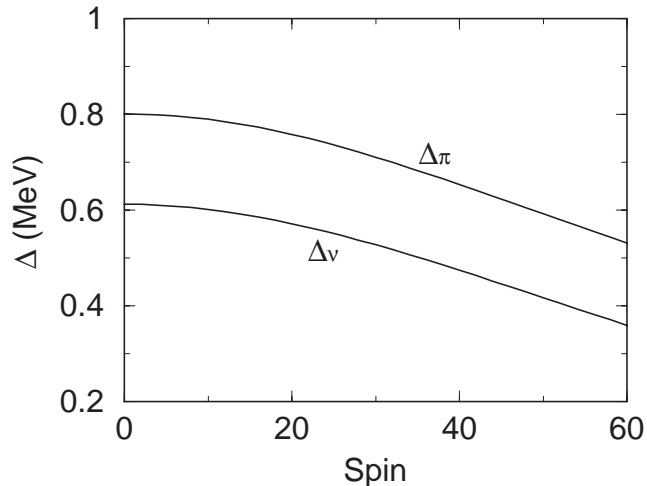


Fig. 4. Calculated (proton and neutron) pairing gaps in the HD states in  $^{110}\text{Pd}$ .

ment. However, our many-body wavefunction does not give a sudden collapse in the pair field, or a phase transition from a superfluid to a normal state. This means that our results suggest that a considerable amount of pairing correlation remains even in the highest spin states in the HD well.

#### 4 Quantitative predictions

We finally present quantitative predictions for yrast energies of the rotational bands (the lowest state at each angular momentum) in  $^{110}\text{Pd}$  at each of the minima. In Fig. 5,  $\gamma$ -ray energies are calculated by the PSM with the basis deformation  $\varepsilon_2 = 0.25$  for the ND band,  $\varepsilon_2 = 0.57$  for the SD band, and  $\varepsilon_2 = 0.79$  for the HD band, respectively. The experimental ND yrast band in this nucleus is also shown for comparison. To support the prediction, the PSM results for the two experimentally-known bands in  $^{108}\text{Cd}$  are also calculated by using the same calculation condition. As one can see, our results agree well with the known ND band in  $^{110}\text{Pd}$ , as well as with the known ND and the highly deformed band in  $^{108}\text{Cd}$ . The SD and HD bands in  $^{110}\text{Pd}$  are our predictions, awaiting experimental confirmation.

We have also carried out systematical calculations for the Zr, Mo, Ru, Pd, and Cd isotopes. Our results indicate that some isotopes of Zr, Mo, Ru, Pd, and Cd, with the neutron number around 64, show separate minima corresponding to SD and HD shapes. For all these nuclei, a SD minimum is found at  $\varepsilon_2 \approx 0.56$  starting from  $I \approx 24$ , and a HD one at  $\varepsilon_2 \approx 0.80$  from  $I \approx 44$ . These predictions are obtained based on a theory that has quantitatively described the observed band in  $^{108}\text{Cd}$  [9,11], which, according to our present results, lies just a step away from the mass region exhibiting hyper-deformed shapes.

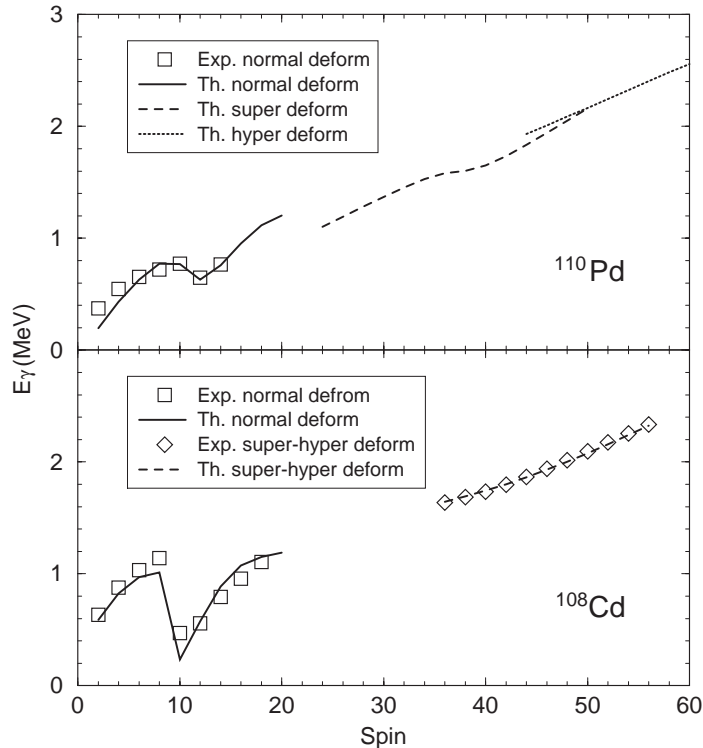


Fig. 5. Calculated  $\gamma$ -ray energies ( $E_\gamma(I) = E(I) - E(I-2)$ ) for  $^{110}\text{Pd}$  (upper panel) at different energy minima shown in Fig. 1. The theoretical results are compared with available ND data. Those for SD and HD states in  $^{110}\text{Pd}$  are predictions. Results for  $^{108}\text{Cd}$  (lower panel) are also given, and compared with known data.

## 5 summary

To summarize, using the projection method implemented in the Projected Shell Model, we have performed energy surface calculations for the A-110 mass region. Our results for  $^{110}\text{Pd}$  have indicated that three distinct energy minima, occurring at different angular-momentum regions, coexist in one nucleus. We have further investigated the source for the occurrence of these minima. The exact treatment of nuclear rotation through angular momentum projection can be important because the shapes in this study appear as sensitive functions of angular momentum (e.g. the rapid shape change in low-spin states at the ND minimum and the emergence of SD and HD minimum at sufficiently high-spins). Pairing correlation is sustained in our wavefunctions even at the highest spin of the HD states. Detailed analysis has shown that, while the nucleons occupying the high- $j$  intruder orbitals have a larger amount of individual contributions to the total collectivity, the major part of collectivity is originated from the rest normal orbitals.

Based on the present study, we have suggested that several nuclei in the A-110 mass region, with the neutron number around 64, would be the promising

candidates in which long-anticipated hyper-deformed rotational bands may be observed. Thus, the present work has shown a picture of coexistence of three distinct deformation minima, corresponding to normal, super-, and hyper-deformed shapes, in nuclei. We hope that these predictions can be experimentally confirmed in the near future.

This work was supported partially by the Chinese Major State Basic Research Development Program through grant 2007CB815005, by U.S. NSF under contract PHY-0216783 (Y.S.), by U.S. DOE under contract DE-FG02-96ER40983 (J.-y.Z.), and by NNSF of China under contract 10325521 (G.-L.L.).

## References

- [1] A. Bohr and B. R. Mottelson, *Nuclear Structure* (W.A. Benjamin, Inc., New York, 1975).
- [2] P. J. Nolan and P.J. Twin, *Ann. Rev. Nucl. Part. Sci.* **38** (1988) 533.
- [3] J. Dudek, T. Werner, and L. L. Riedinger, *Phys. Lett. B* **211** (1988) 252.
- [4] T. Werner and J. Dudek, *At. Data Nucl. Data Tables* **59** (1995) 1.
- [5] R. R. Chasman, *Phys. Rev. C* **64** (2001) 024311.
- [6] B. Buck, A. C. Merchant, and S. M. Perez, *Phys. Rev. C* **65** (2002) 067306.
- [7] A. Galindo-Uribarri *et al.*, *Phys. Rev. Lett.* **71** (1993) 231;  
D. R. LaFosse *et al.*, *Phys. Rev. Lett.* **74** (1995) 5186;  
G. M. Ter-Akopian *et al.*, *Phys. Rev. Lett.* **77** (1996) 32;  
A. Krasznahorkay *et al.*, *Phys. Rev. Lett.* **80** (1998) 2073.
- [8] J. Dudek, N. Schunck, and N. Dubray, *Acta Phys. Polon.* **36**, 975 (2004);  
P. Fallon, *Acta Phys. Polon.* **36**, 1003 (2004);  
H. Hübel, *Acta Phys. Polon.* **36**, 1015 (2004);  
B. M. Nyako *et al.*, *Acta Phys. Polon.* **36**, 1033 (2004).
- [9] R. M. Clark *et al.*, *Phys. Rev. Lett.* **87** (2001) 202502.
- [10] K. Hara and Y. Sun, *Int. J. Mod. Phys. E* **4** (1995) 637.
- [11] C.-T. Lee, Y. Sun, J.-y. Zhang, M. Guidry, and C.-L. Wu, *Phys. Rev. C* **65** (2002) 041301(R).
- [12] P. Ring and P. Schuck, *The Nuclear Many-Body Problem* (Springer, New York, 1980).
- [13] Y. Sun and M. Guidry, *Phys. Rev. C* **52** (1995) R2844.
- [14] Y. Sun, J.-y. Zhang, and M. Guidry, *Phys. Rev. Lett.* **78** (1997) 2321.

- [15] Y. Sun, J.-y. Zhang, M. Guidry, and C.-L. Wu, Phys. Rev. Lett. **83** (1999) 686.
- [16] G.-L. Long and Y. Sun, Phys. Rev. C **63** (2001) 021305(R).
- [17] A. Hayashi, K. Hara, and P. Ring, Phys. Rev. Lett. **53** (1984) 337.
- [18] J. L. Egido, L. M. Robledo, and Y. Sun, Nucl. Phys. A **560** (1993) 253.
- [19] J. L. Egido and L. M. Robledo, Lect. Notes Phys. **641** (2004) 269.
- [20] T. Niksic, D. Vretenar, and P. Ring, Phys. Rev. C **73** (2006) 034308.
- [21] K.-I. Enami, K. Tanabe, N. Yoshinaga, and K. Higashiyama, Prog. Theor. Phys. **104** (2000) 757.
- [22] A. Valor, P.-H. Heenen, and P. Bonche, Nucl. Phys. A **671** (2000) 145.
- [23] T. Bengtsson and I. Ragnarsson, Nucl. Phys. A **436** (1985) 14.
- [24] P. H. Regan *et al.*, Phys. Rev. Lett. **90** (2003) 152502.
- [25] Details will be published elsewhere.
- [26] J. Dudek, W. Nazarewicz, Z. Szymanski, and G. A. Leander, Phys. Rev. Lett. **59** (1987) 1405.
- [27] J. Dudek, K. Pomorski, N. Schunck, and N. Dubray, Eur. Phys. J. A **20** (2004) 15.
- [28] N. Schunck, J. Dudek, and B. Herskind, Phys. Rev. C **75** (2007) 054304.